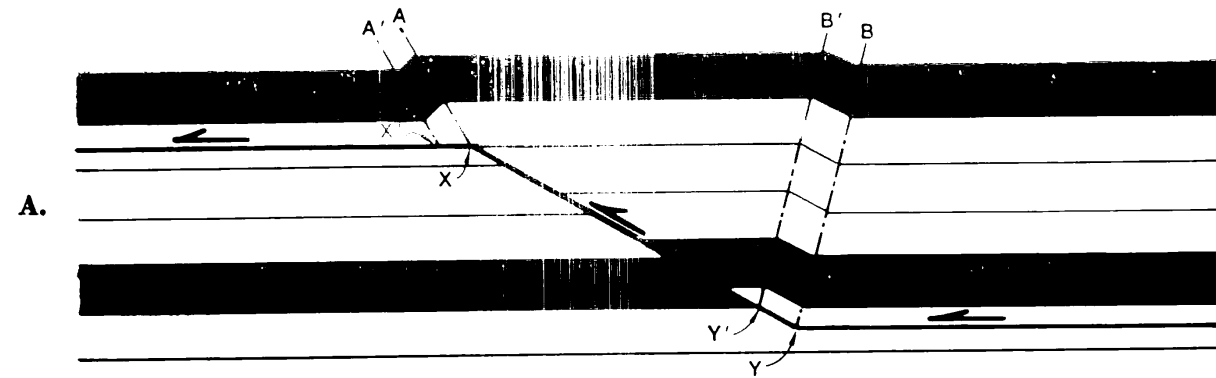


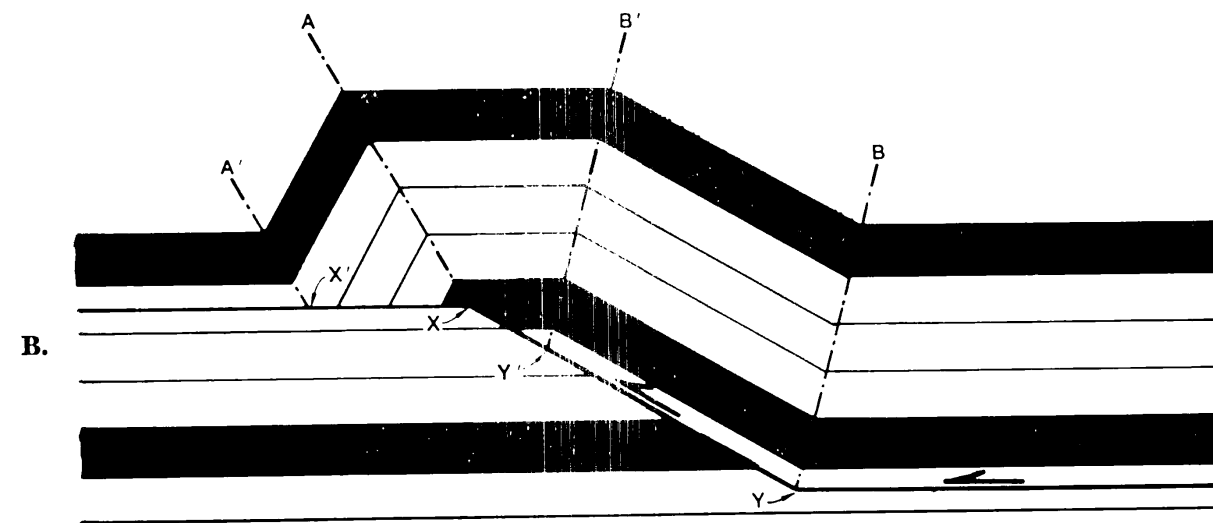
Retrodeformable Sections in Fold-Thrust Belts

Fault-bend fold

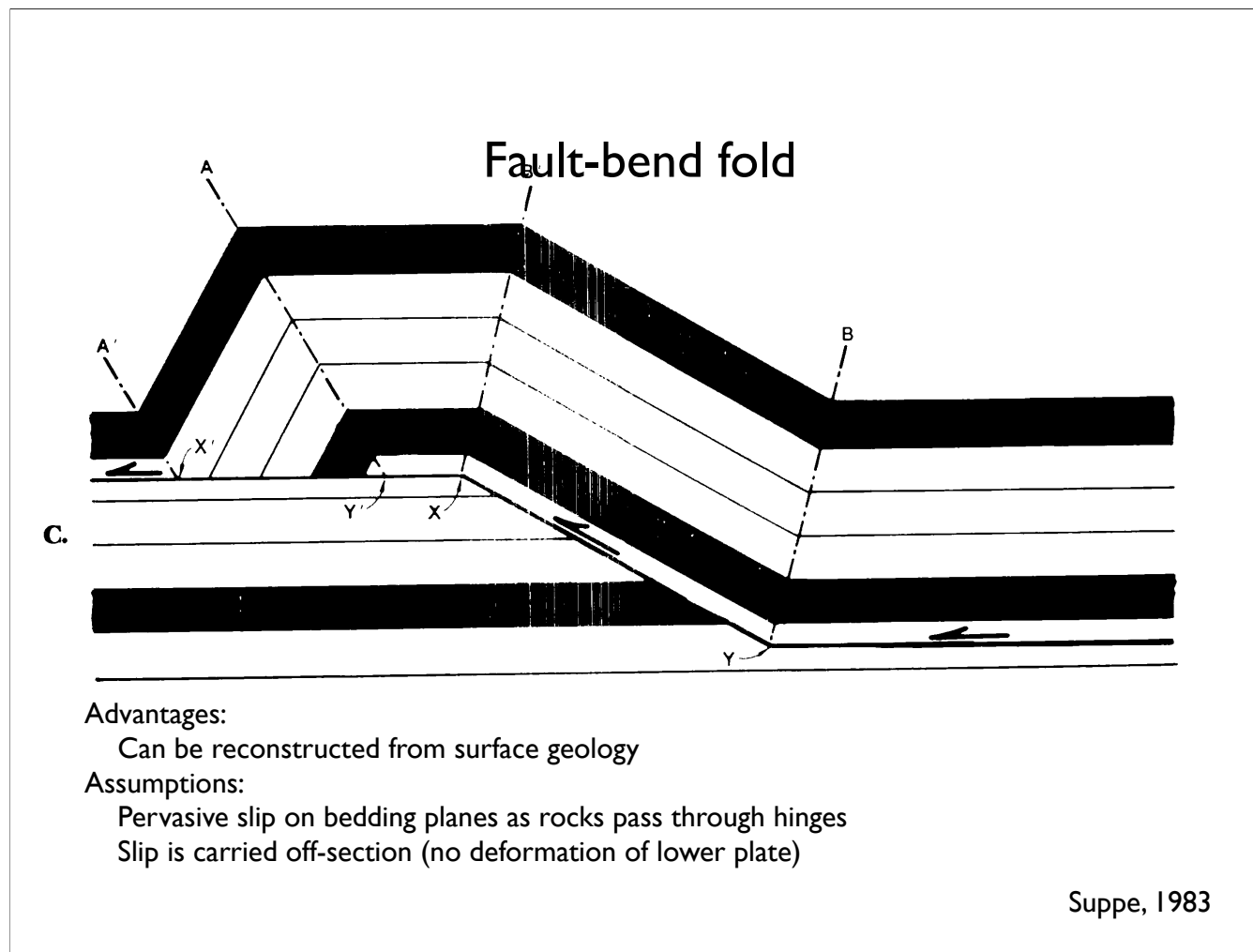


Suppe, 1983

Fault-bend fold

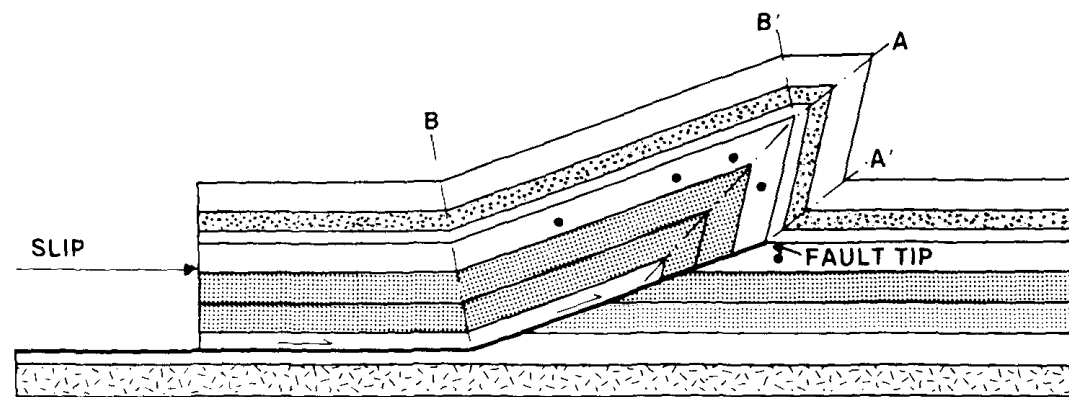


Suppe, 1983



This style is usually looking to balance line lengths (length of a bed).

Fault-Propagation fold



Namson and Davis, GSA Bull , 1988 after Suppe and Medwedeff, 1984

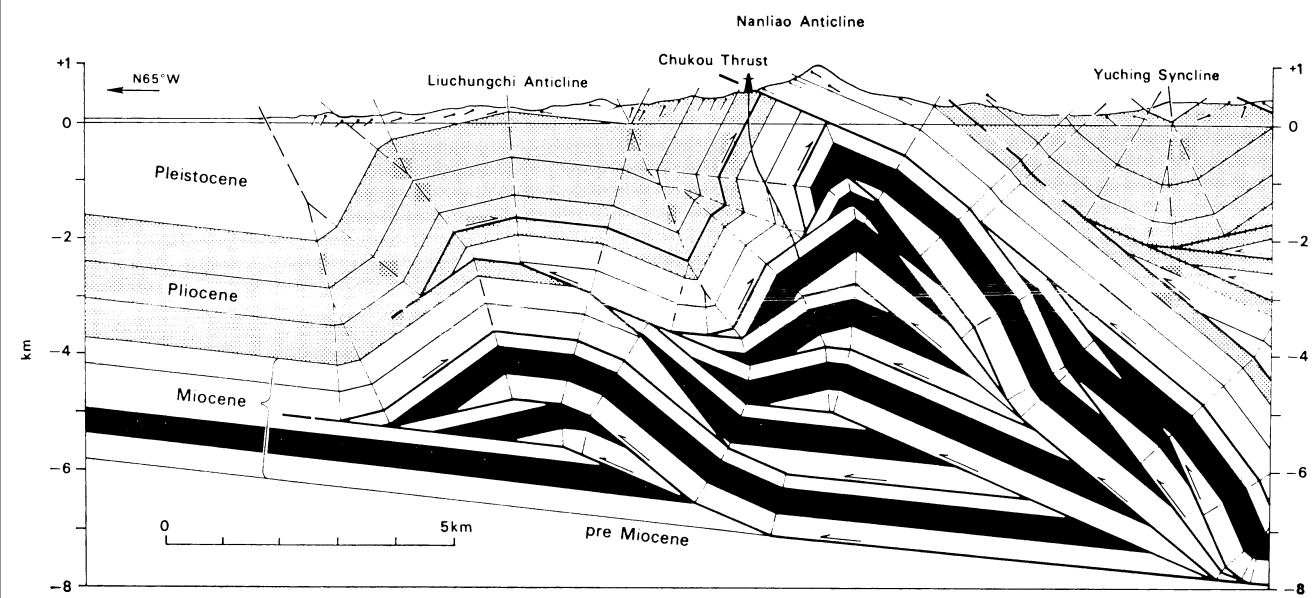
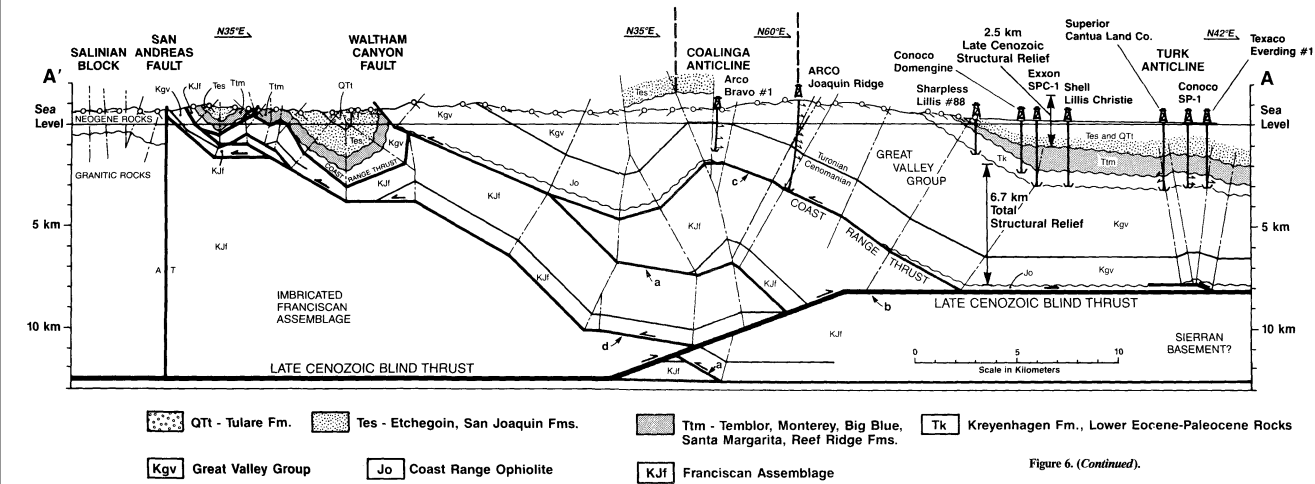


Fig. 24. Structural interpretation of the Nanliao anticline, southern Taiwan (modified from Suppe, 1980b).

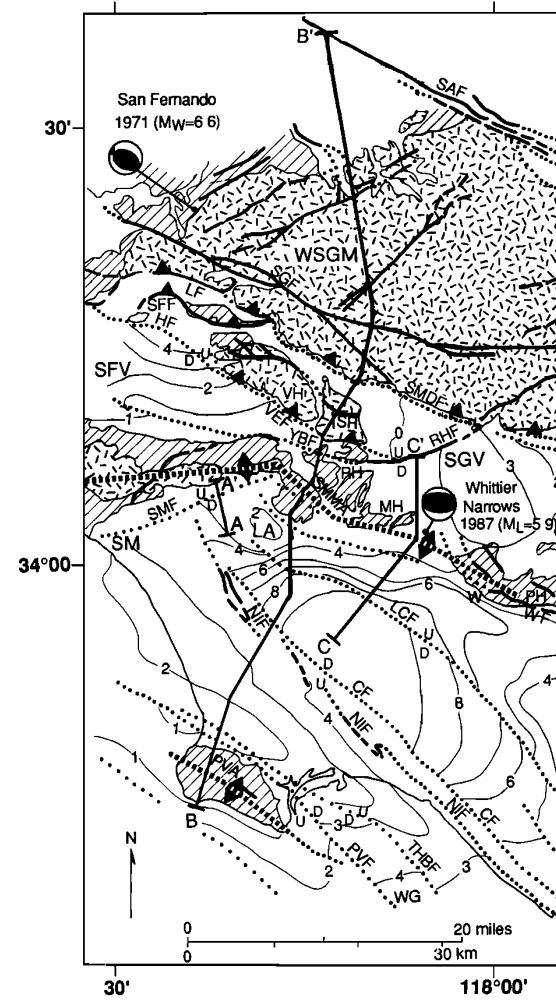
Suppe, 1983

Coalinga, California (site of 1983 earthquake)

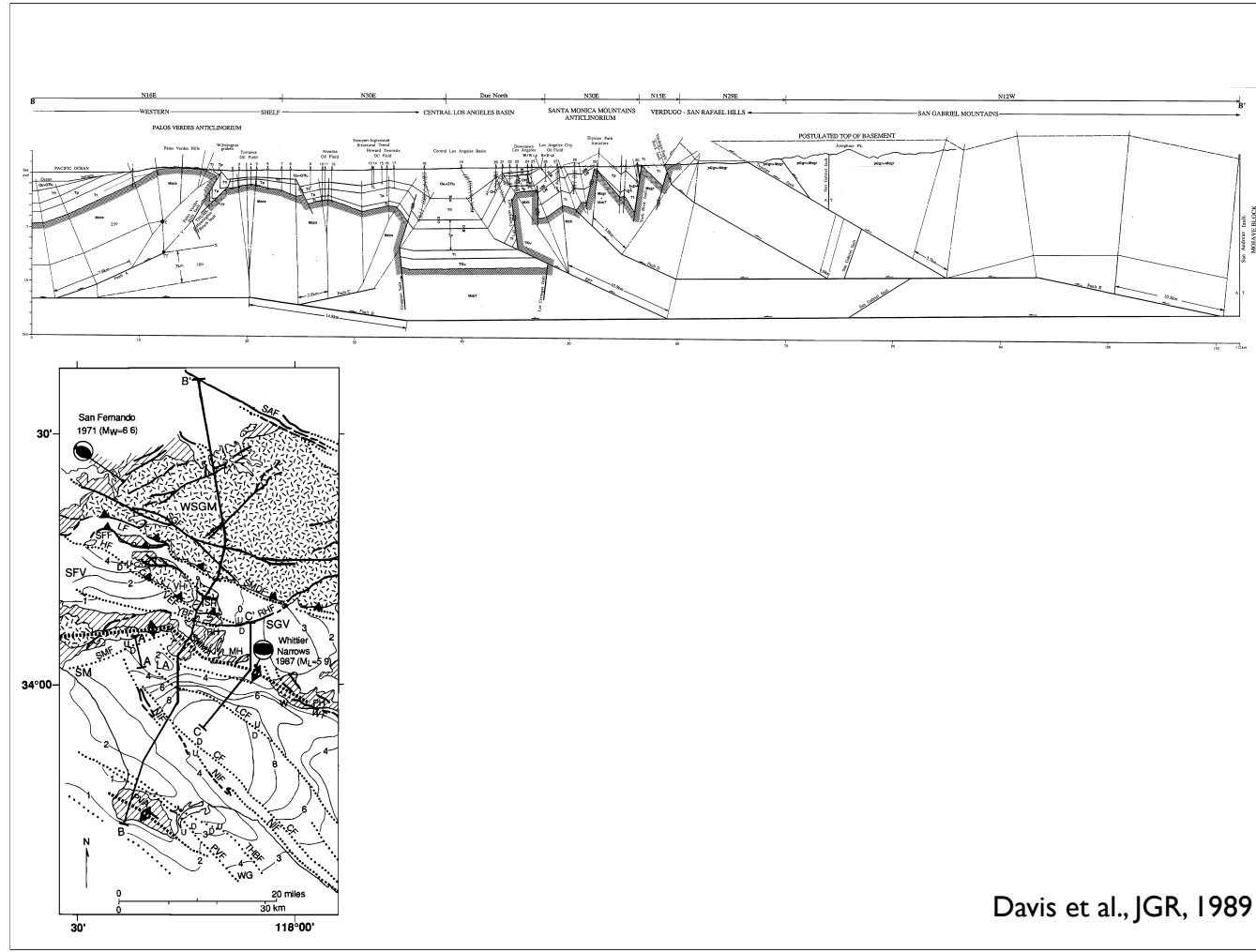


Namson and Davis, GSA Bull , 1988

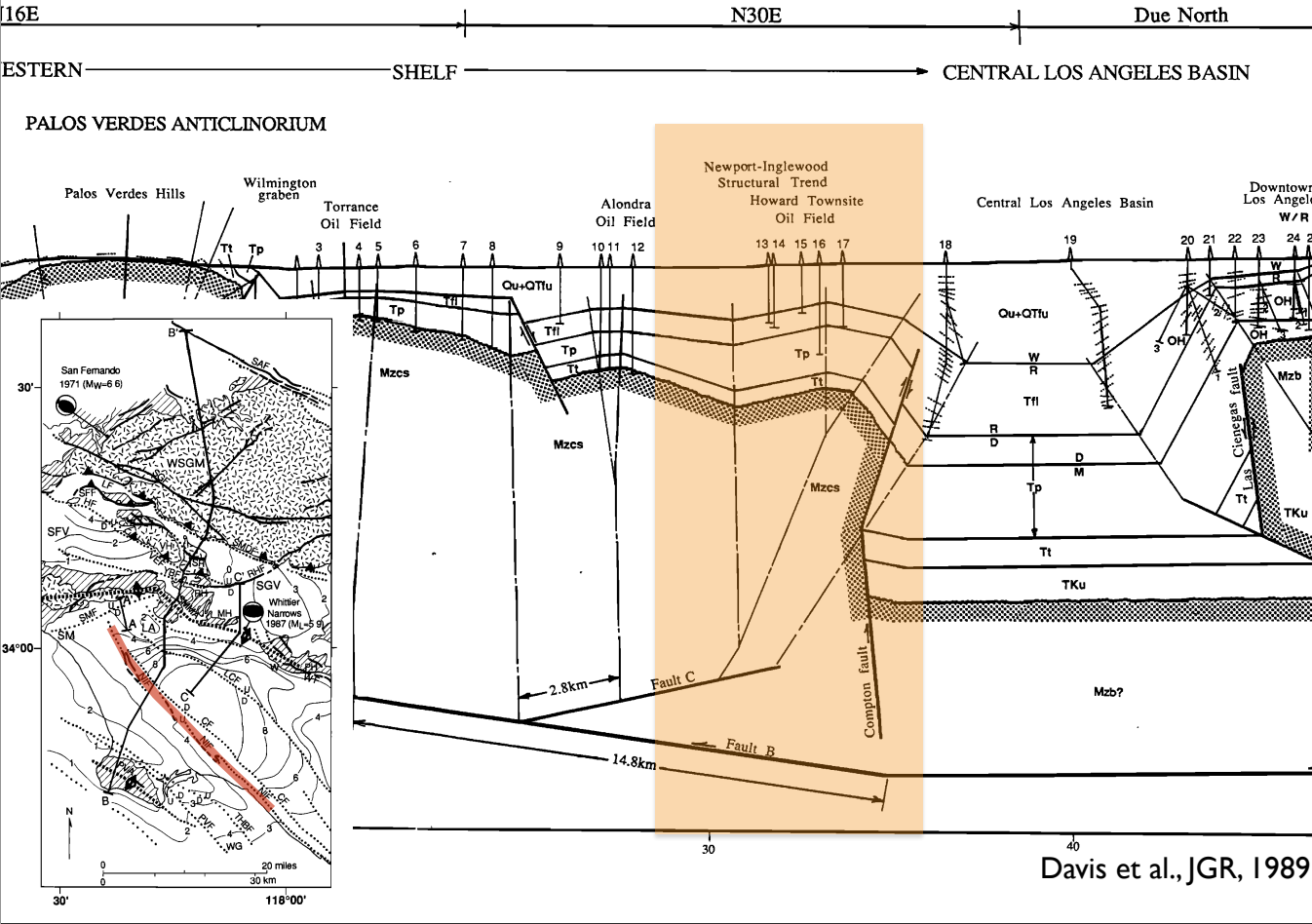
Coalinga anticline grew in the earthquake, which lacked any surface faulting.

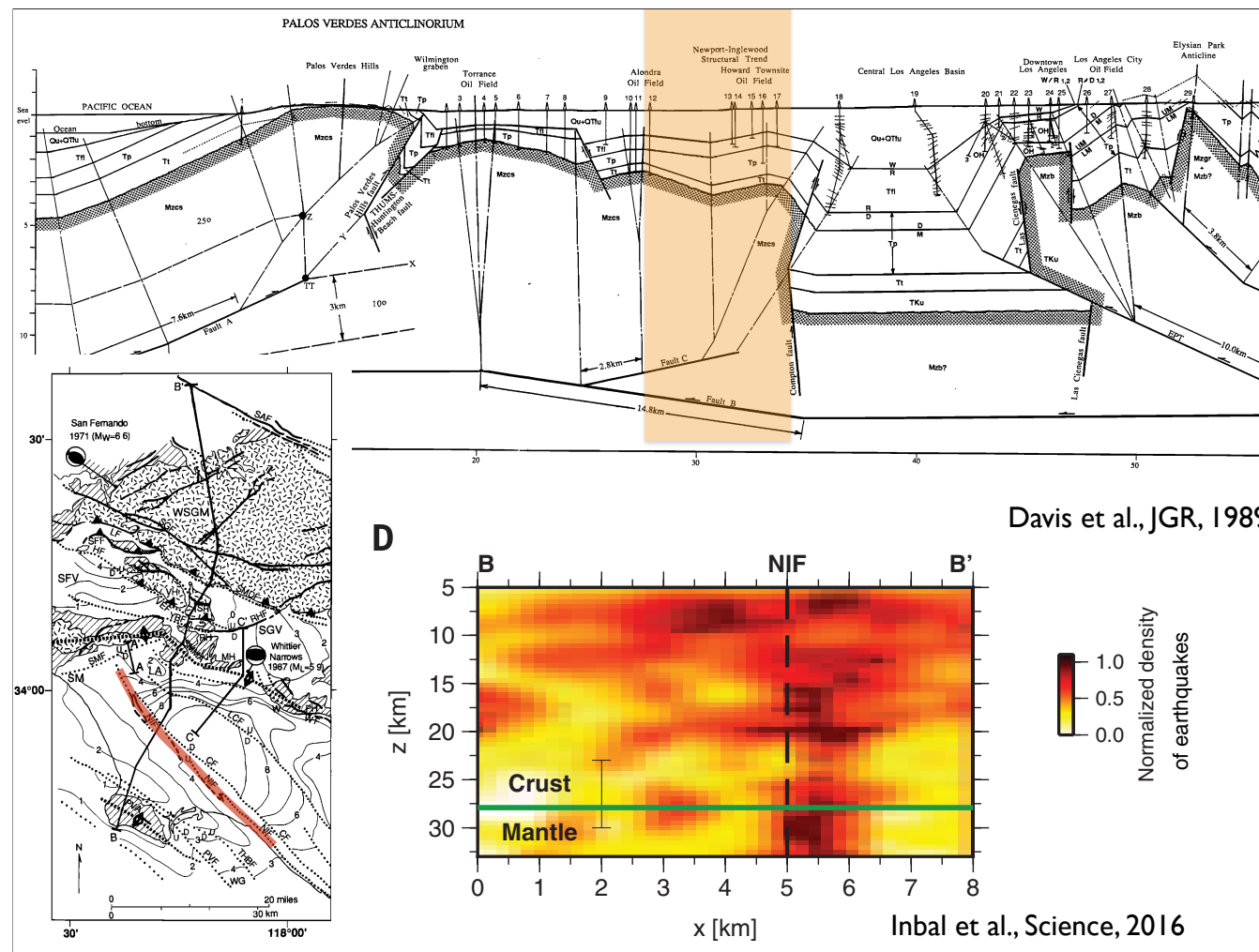


Davis et al., JGR, 1989

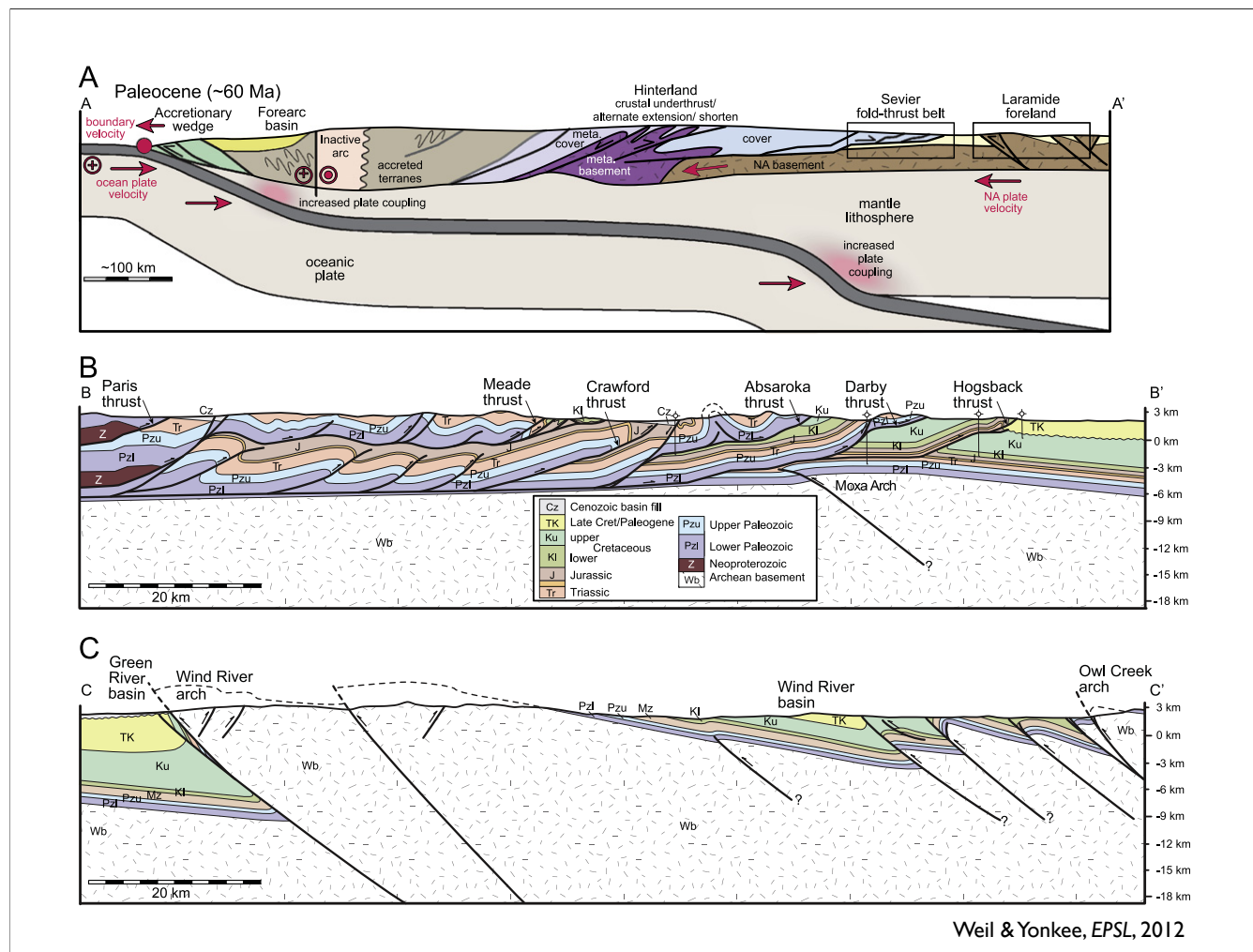


Davis et al., JGR, 1989





Inbal et al. got lots of small EQs from a very dense array and see the Newport–Inglewood fault extending into the mantle, not detached as thought by Davis et al. This helps reveal a weakness of the geometric reconstructions of fold belts: they need detachment to go off the edge of the model at the side.



So we'll transition from the Sevier to the Laramide. Consider what these faults do at depth—what is the basis for this. Note difference in thickness of the units on thrusts to west vs foreland to east.

Fault geometry in basement-cored uplifts

FORELAND STRUCTURAL MODELS

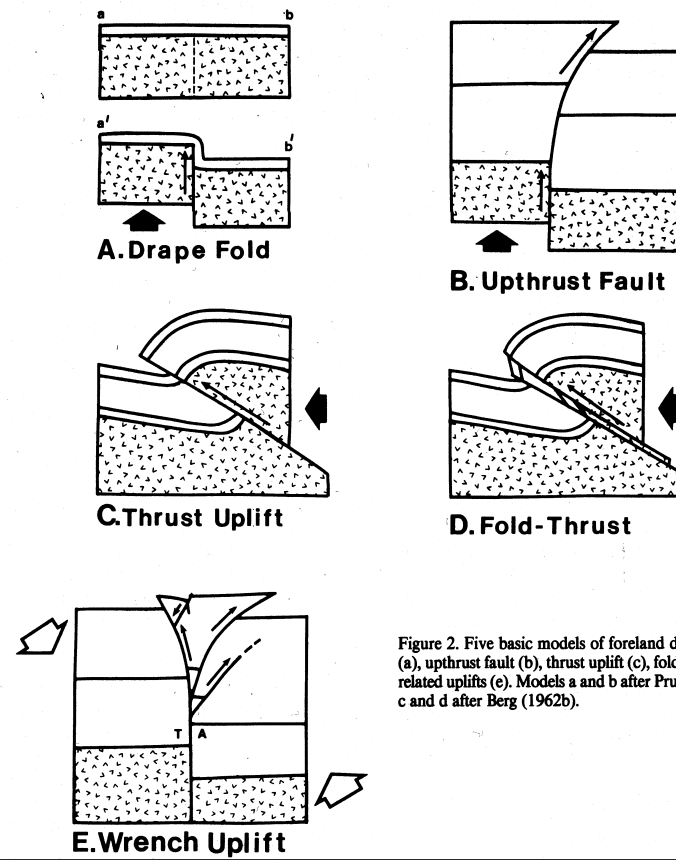


Figure 2. Five basic models of foreland deformation are the drape fold (a), upthrust fault (b), thrust uplift (c), fold-thrust uplift (d), and wrench-related uplifts (e). Models a and b after Prucha and others (1965); models c and d after Berg (1962b).

Brown, GSA Mem 171, 1988

Well, as a prelude to the Laramide, let's discuss a different flavor of this: basement cored folds.

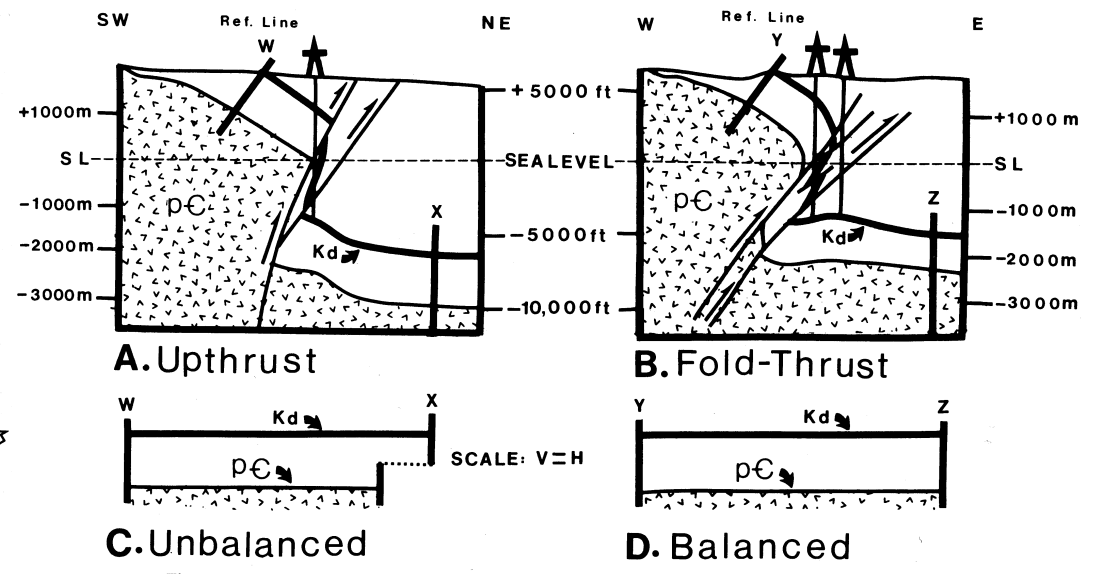
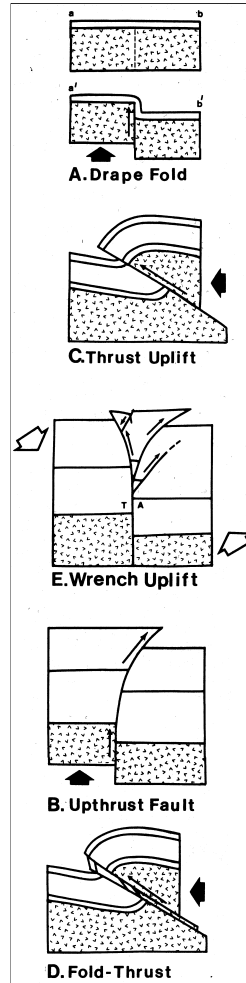
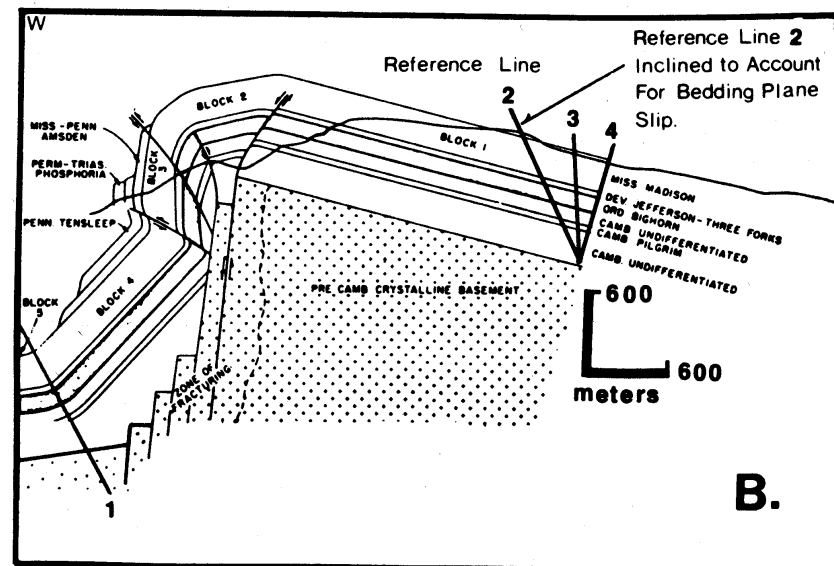
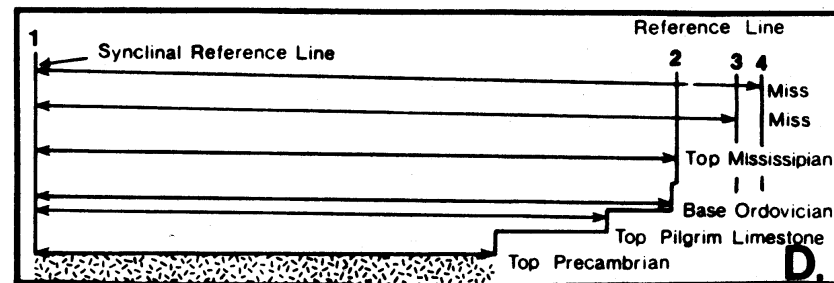


Figure 5. A comparison of interpretations of the Soda Lakes area, Colorado, utilizing the upthrust model (a) modified from Osterwald (1961), and the fold-thrust model (b) modified from Berg (1962a). Comparison of bed-length measurements of the Dakota Sandstone (Kd) and the top of the Precambrian basement between reference lines (W-X), and (Y-Z), indicates the upthrust model (c) is out of structural balance by approximately 20 percent, whereas the fold-thrust model (d) is balanced to less than 5 percent error (after Brown, 1987).

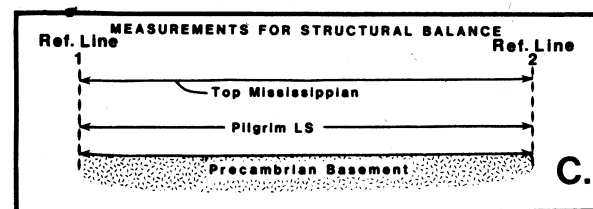
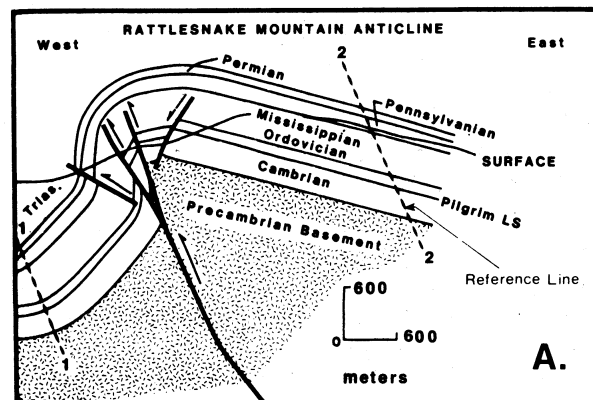


Rattlesnake Mtn
interpretation of
Sterns, 1971

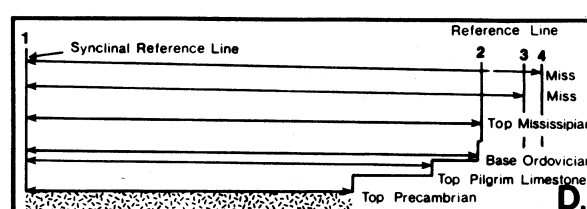
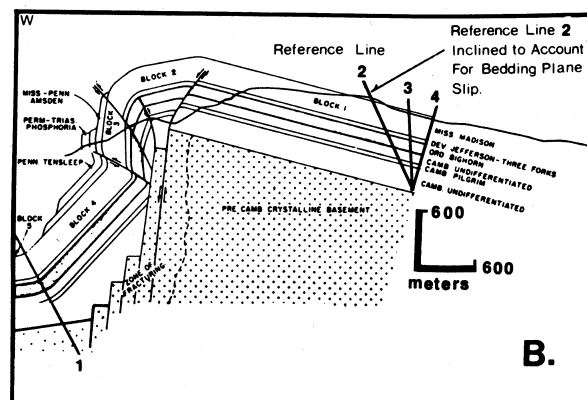


Brown, GSA Mem 171, 1988

Problems with high-angle (near vertical) faulting to make these uplifts: cannot balance line lengths.



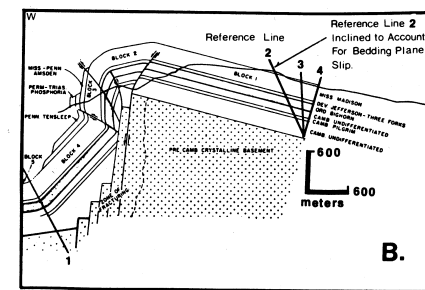
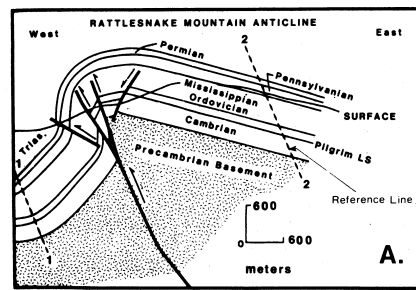
Rattlesnake Mtn
interpretation of
Brown, 1984



Rattlesnake Mtn
interpretation of
Sterns, 1971

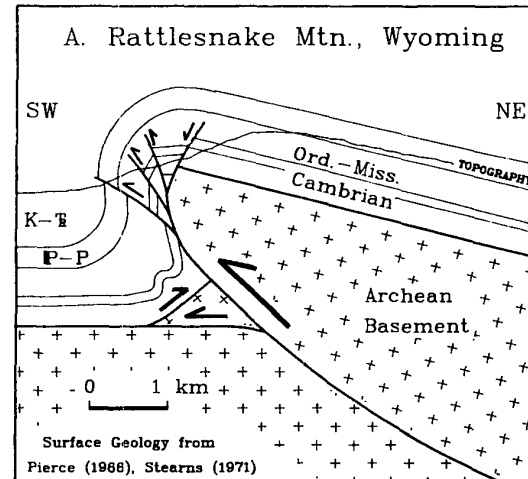
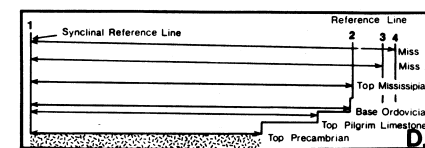
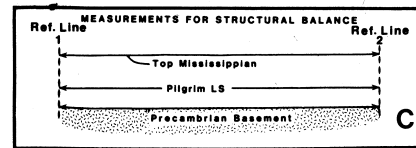
Brown, GSA Mem 171, 1988

Rattlesnake Mtn interpretation of Brown, 1984

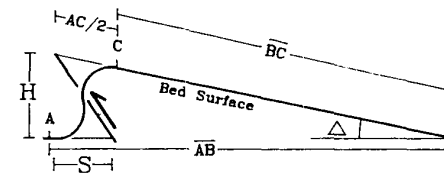


Rattlesnake Mtn interpretation of Sterns, 1971

Rattlesnake Mtn interpretation of Erslev, 1986



B. Fault Dip Calculation



$$\begin{aligned} \Delta &= \text{Hanging Wall Dip} - \text{Footwall Dip} \\ AC \text{ and } AB &\text{ Are Bed Lengths} \\ H &= (\overline{BC} + AC/2) \sin \Delta \\ S &= \text{Total Shortening} - \text{Tilt Shortening} \\ S &= AB - \overline{AB} - (\overline{BC} + AC/2) (1 - \cos \Delta) \\ \text{Fault Dip Relative to Footwall} &= \arctan (H/S) \end{aligned}$$

Erslev, Geology, 1986

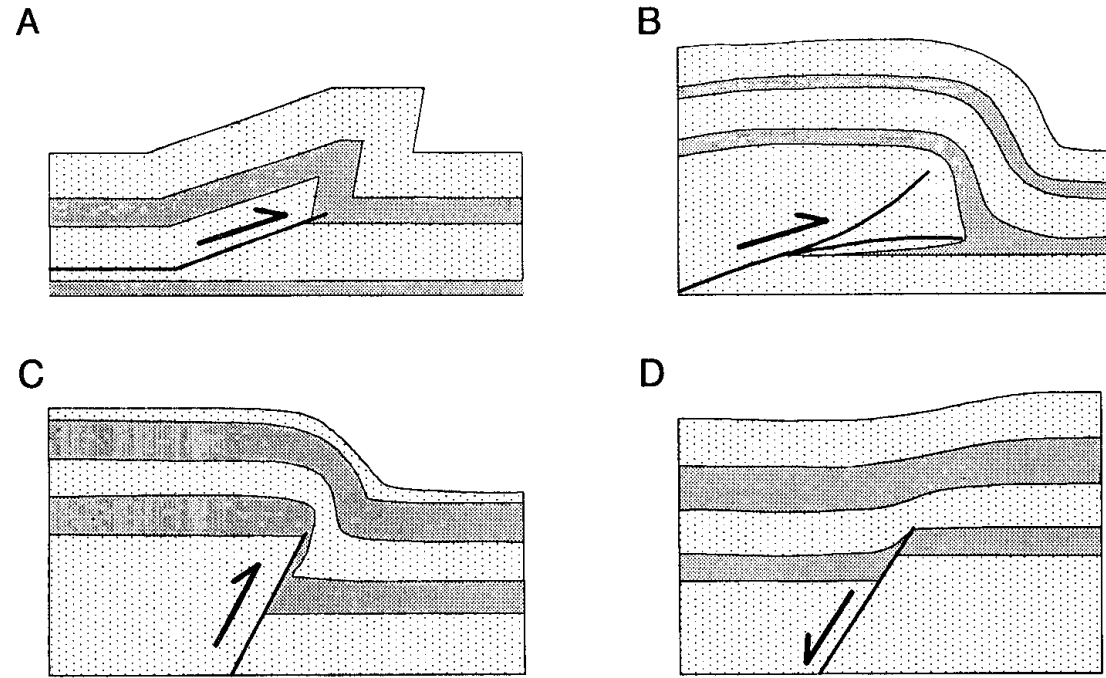


Figure 1. Models of fault-propagation folds. A: Geometric kink-band model (Suppe and Medwedeff, 1984). B, C, D: Analog experimental models of folds above thrust (B; Chester et al., 1988), reverse (C; Friedman et al., 1980), and normal (D; Withjack et al., 1990) faults.